processes

MDPI

Article

Design of Cross-Linked Starch Nanocapsules for Enzyme-Triggered Release of Hydrophilic Compounds

Fernanda R. Steinmacher [1,2], Grit Baier [2], Anna Musyanovych [2,3], Katharina Landfester [2], Pedro H. H. Araújo [1] and Claudia Sayer [1,*]

1 Chemical Engineering and Food Engineering Department, Federal University of Santa Catarina—UFSC, CP 476, Florianópolis 88040-900, Brazil; fersteinmacher@gmail.com (F.R.S.); pedro.h.araujo@ufsc.br (P.H.H.A.)
2 Max Planck Institute for Polymer Research, Ackermannweg 10, 55128 Mainz, Germany; grit.baier@online.de (G.B.); Anna.Musyanovych@imm.fraunhofer.de (A.M.); landfest@mpip-mainz.mpg.de (K.L.)
3 Nanoparticle Technologies Department, Fraunhofer ICT-IMM, Carl-Zeiss-Str. 18-20, 55129 Mainz, Germany
* Correspondence: claudia.sayer@ufsc.br; Tel.: +55-48-3721-2516

Academic Editor: Alexander Penlidis
Received: 8 March 2017; Accepted: 2 May 2017; Published: 6 May 2017

Abstract: Cross-linked starch nanocapsules (NCs) were synthesized by interfacial polymerization carried out using the inverse mini-emulsion technique. 2,4-toluene diisocyanate (TDI) was used as the cross-linker. The influence of TDI concentrations on the polymeric shell, particle size, and encapsulation efficiency of a hydrophilic dye, sulforhodamine 101 (SR 101), was investigated by Fourier transform infrared (FT-IR) spectroscopy, dynamic light scattering (DLS), and fluorescence measurements, respectively. The final NC morphology was confirmed by scanning electron microscopy. The leakage of SR 101 through the shell of NCs was monitored at 37 °C for seven days, and afterwards the NCs were redispersed in water. Depending on cross-linker content, permeable and impermeable NCs shell could be designed. Enzyme-triggered release of SR 101 through impermeable NC shells was investigated using UV spectroscopy with different α-amylase concentrations. Impermeable NCs shell were able to release their cargo upon addition of amylase, being suitable for a drug delivery system of hydrophilic compounds.

Keywords: inverse mini-emulsion; interfacial polymerization; aqueous-core nanocapsules; high-efficiency encapsulation; enzyme-triggered release

1. Introduction

The development of new strategies for the delivery of hydrophilic drugs is emerging as an important research field [1–6] due to several facts: water-soluble drugs are often easily degradable in the body, poor cellular penetration of macromolecules, toxicity of small molecules, and unsuitable biodistribution [1]. These limitations can be overcome by the use of nanocarriers that offer protection against degradation or oxidation until the drugs reach the targeted tissues.

The importance of polymeric nanoparticles is now widely recognized in order to conceive drug carriers and controlled-release systems due to their versatility and unique features, such as different compositions, morphologies, reduced particle sizes and high surface area, allowing surface modification [7] in order to design the triggered release, for example, pH-responsive [8] and enzyme-responsive nanoparticles [9,10]. Thus, compounds, materials and, especially, the surface of drug carriers should be biocompatible, nontoxic and, sometimes, also biodegradable [11]. Therefore,

the use of well-known polysaccharides for the preparation of drug delivery systems has advantages regarding safety, toxicity, and availability [12,13].

Recently, starch-based nanocapsules prepared by the emulsion solvent evaporation method were used for topical application and showed very good skin compatibility, an absence of allergenic potential and, additionally, improved skin permeation of lipophilic bioactive molecules [13]. However, regarding oral administration, starch-based drug delivery systems experience different environments in the body, especially, environmental conditions that favor enzymatic biodegradation. Although amylase is the major component of parotid saliva, most degradation of starch results from pancreatic enzymes in the small intestine, and not from salivary amylases [14–16]. Efforts have been made to inhibit or reduce the enzymatic degradation. In this way, starch-based nanoparticles have been obtained using modified [17] and cross-linked starch [18].

Well-established methods usually used for the encapsulation of lipophilic compounds result in low encapsulation efficiency of hydrophilic molecules, due to the rapid partitioning of the drug to the external aqueous phase [4]. Double-emulsion solvent diffusion techniques and emulsion solvent evaporation are the most common methods used for the encapsulation of hydrophilic compounds in nanoparticles, but usually result in low encapsulation efficiency [4,19]. Higher loading efficiency of hydrophilic compounds was recently reported using a novel organic solvent-free double-emulsion/melt dispersion technique [5].

High encapsulation efficiency of hydrophilic drugs was achieved using the inverse mini-emulsion polymerization technique. The high stability of droplets/particles created by the mini-emulsion technique allows performing the polymerization reaction inside the droplet, as well as at their interface [20]. A relatively recent strategy is the use of interfacial polymerization, which allows the preparation of aqueous-core nanocapsules. Polyurea, polythiourea, or polyurethane shells were successfully obtained by interfacial polyaddition at the droplet interface using starch, dextran, 1,6-hexanediol, and 1,6-diaminohexane, for example [2,3,18,21,22]. The core composed of water optimizes the drug solubility inside the nanoparticle, providing high encapsulation efficiency.

NaCl is the most common salt applied in inverse mini-emulsion polymerization, although hydrophilic metal salts composed of transition metal cations, such as Fe^{2+}, Fe^{3+}, Co^{2+}, Ni^{2+}, and Cu^{2+}, may present advantages for further application [23]. Copper (Cu) is an element essential for almost all organisms, including bacteria, but Cu overload is toxic in most systems. Studies show Cu accumulates in macrophage phagosomes infected with bacteria, suggesting that Cu is mobilized in mammals to control bacterial growth [24]. In fact, Wolschendorf et al. [25] found that dietary supplementation with Cu resulted in the accumulation of Cu in lung granulomas of *Mycobacterium tuberculosis*-infected guinea pigs, and coincided with a reduction in the bacterial burden.

The effective carrier for drug delivery should be optimized in terms of chemical composition, surface morphology, size, shape, and be able to release its payload in a controlled/predictable manner. Therefore, it is of great importance to have knowledge about how the chemical compositions affect the degradation kinetics of the carriers in order to program the properties of a carrier during the synthesis for each particular application. Hamdi and Ponchel [26] synthesized starch microspheres using epichlorohydrin as a crosslinking agent, and studied enzymatic degradation by α-amylase. It was suggested that degradation profiles were dependent on the initial size distribution of the microspheres. The aim of this study was to prepare starch nanocapsules by interfacial inverse (water-in-oil) mini-emulsion polymerization using 2,4-toluene diisocyanate as a cross-linker and to evaluate the permeability of the capsule's shell upon enzyme (amylase) degradation by adjusting the chemical parameters during the crosslinking reaction. Our focus was also to evaluate whether the permeability of NC shells can be modulated by the encapsulation of a small hydrophilic molecule, sulforhodamine 101 (SR 101), in aqueous-core NCs for different amounts of cross-linker.

2. Materials and Methods

2.1. Materials

For the synthesis of starch NCs, all chemicals were used without further purification. Hydrophilic potato starch and 2,4-toluene diisocyanate (TDI) were purchased from Fluka (Neu-Ulm, Germany) and Sigma Aldrich (Steinheim, Germany), respectively. Cyclohexane (Sigma Aldrich, Steinheim, Germany) was used as continuous phase. Sodium chloride (NaCl, VWR, BDH Prolabo, Darmstadt, Germany) and copper II sulfate pentahydrate ($CuSO_4 \cdot 5H_2O$, Cromoline, Diadema, Brazil) were used as osmotic costabilizers of the mini-emulsion droplets. Polyglycerol polyricinoleate (PGPR, *Mw* = 5870 g/mol, DANISCO, Kopenhagen, Denmark) was employed as a hydrophobic surfactant. Sulforhodamine 101 (SR 101, *Mw* = 606.71 g/mol, BioChemica, Aldrich, Taufkirchen, Germany) was used as a hydrophilic dye. Sodium dodecyl sulfate (SDS, Merck, Darmstadt, Germany) and Tween 80 (Vetec, São Paulo, Brazil) were used as surfactants to redisperse the cross-linked aqueous-core NCs in the aqueous phase. The α-amylase from *Bacillus subtilis* was purchased from Fluka (Neu-Ulm, Germany). The phosphate buffer solution (PBS at pH 7.4 and 0.05 M) was freshly prepared from monobasic and dibasic sodium phosphate (Vetec, São Paulo, Brazil).

2.2. Preparation of Starch Nanocapsules

Starch nanocapsules (NCs) were prepared by interfacial polymerization by inverse mini-emulsion at 60 °C for 2 h, based on a procedure proposed in the literature [3,18], except for the fact that the dispersed phase was prepared from gelatinizing 0.1 g of starch under stirring for 30 min at 90 °C in a mixture of 50 mg of sodium chloride and 1.3 g of water. When copper salt was used, NaCl was partially replaced by previously-dried $CuSO_4 \cdot 5H_2O$. Subsequently, the macroemulsion was formed by adding the continuous phase, composed of 7.5 g of cyclohexane and PGPR (varied in the range from 10 to 20 wt% related to the disperse phase), to the disperse phase and by stirring over 1 h at room temperature. The mini-emulsion was created by sonication for 3 min at 70% of amplitude in a pulsed regime (20 s on, 10 s pause) using a Branson Sonifier W-450-Digital (Thermo Fisher Scientific, WA, USA) under ice cooling to prevent the evaporation of the continuous phase. A clear solution of cyclohexane (5 g), PGPR (30 mg), and TDI (varied in the range from 80 to 200 mg), previously prepared, was added dropwise to the mini-emulsion for 1 min. The reaction was performed for 2 h at 60 °C or for 24 h at 25 °C, under magnetic stirring. Figure 1 illustrates the different steps. Dye-loaded cross-linked starch NCs were prepared, in brief, replacing the water that composes the dispersed phase by a 0.02 wt% SR 101 aqueous solution.

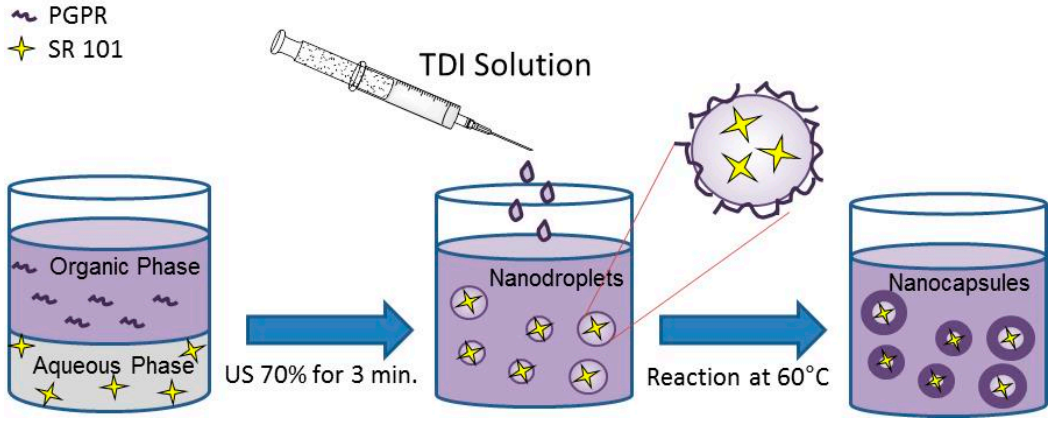

Figure 1. Preparation of aqueous-core NCs by interfacial polymerization via inverse mini-emulsion.

In order to redisperse the NCs in water, the following procedure was applied: 1 g of NCs dispersed in cyclohexane were redispersed in 5 g of 0.3 wt% SDS aqueous solution after 30 min in a sonication

bath (25 kHz) and magnetically stirred at 1000 rpm over 8 h at room temperature for evaporation of the organic solvent.

2.3. Characterization

The intensity average particle size was measured by dynamic light scattering (DLS, NanoSizer Nano S, Malvern, UK) of diluted dispersions. The morphology of the NCs was evaluated by field emission scanning electron microscopy (FESEM) (LEO (Zeiss) 1530 Gemini, Oberkochen, Germany) at an accelerating voltage of 0.5 kV. Generally, the samples were prepared by diluting the NCs in cyclohexane, then one droplet of the sample was placed onto silica wafers and dried under ambient conditions.

Fourier transform infrared (FT-IR) spectroscopy was performed to evaluate the reaction between the cross-linker TDI and hydroxyl groups of starch during the mini-emulsion polymerization. The sample powder was obtained by freeze-drying the particles dispersion for 24 h at −60 °C under reduced pressure. The dried sample was pressed with KBr to form a pellet. Spectra were recorded using a IFS 113v spectrometer (Bruker, Billerica, MA, USA). When mentioned, attenuated total reflectance (ATR) mode was used. For that, a film of the sample was obtained drying the final mini-emulsion in a convection oven at 60 °C and spectra were recorded using a Tensor 27 spectrometer (Bruker, Billerica, MA, USA).

Interfacial tension measurements were carried out by using a series of colloidal dispersions of varying type and amount of hydrophilic salts. The measurements were carried out using a drop shape analysis system (Ramé-hart Model 250 Standard Goniometer/Tensiometer, Ramé-hart, Succasunna, NJ, USA). The equipment was calibrated by measuring the pure air-water surface tension until a value of 72.8 mN m^{-1} was obtained. Single droplets (50 μL) of the dispersed phase were formed at the end of a steel needle (1.84 mm), placed in the oil phase within a cuvette, and images were recorded using a digital camera over a period of time at 21 °C. The profile of the droplet in each image was detected automatically using the analysis software package and fitted to the Young-Laplace equation to obtain interfacial tension values as a function of time. At least three independent measurements were taken.

The encapsulation efficiency was studied using a fluorescence spectrometer (NanoDrop ND-3300, Thermo Fisher Scientific, WA, USA) after redispersion of NCs in water. SR 101 was chosen as the hydrophilic fluorescent dye due its stable fluorescence (red fluorophore λexc/em: 583/603 nm) during polymerization. Sonication and exposition to different temperatures did not influence the intensity of its fluorescence signal. After the synthesis step, NCs dispersed in cyclohexane were freeze-dried, and the encapsulation efficiency was determined by redispersing 15 μg of the dried sample in 1 g of 0.3 wt% SDS aqueous solution. The NCs were collected by centrifugation for 20 min at 10,000 rpm. The fluorescence signal of the supernatant related to a calibration curve provided the concentration of unloaded dye. The encapsulation efficiency (EE (%)) was calculated as the difference between total concentration of dye in the sample ($W_{total,sample}$) and the concentration of free dye (W_{free}) using the following equation:

$$EE\ (\%) = \frac{\left(W_{total,sample} - W_{free}\right)}{W_{total,sample}} \times 100 \quad (1)$$

The encapsulation efficiency of the dye after redispersion, and the leakage by migration of the hydrophilic dye to the continuous aqueous phase, were calculated by relating the fluorescence signal of the supernatant obtained from the sample after centrifugation at 4000 rpm for 30 min. The leakage of SR 101 was monitored for seven days at 37 °C. Aliquots were taken at certain times and centrifuged at 4000 rpm for 30 min. The fluorescence signal of the supernatant related to a calibration curve provided the concentration of non-entrapped dye (W_{free}). The cumulative loss of SR 101 ($1 - EE$ (%)) was calculated using the following equation:

$$1 - EE\,(\%) = \frac{\left(W_{free}\right)}{W_{total,sample}} \times 100 \quad (2)$$

where $W_{total,sample}$ stands for the total concentration of dye in the sample. All experiments were repeated three times and for each sample the encapsulation efficiency was calculated from two measurements.

The activity of α-amylase was determined based on colorimetric measurements at 37 °C and pH 7.4, 0.05 M PBS. The reaction was started by adding 0.5 mL of α-amylase solution to 10 mL of gelatinized 0.1 g/mL starch solution in pH 7.4 and 0.05 M PBS. The final enzyme concentration was 3.61 µg/mL of α-amylase. The reaction was allowed to proceed at 37 °C and stopped by adding 0.5 mL of reacted starch dispersion to 5 mL of 0.1 M HCl solution, and 0.5 mL of the terminated reaction solution was added to 5 mL of iodine reagent (0.2% iodine and 2% potassium iodine) aqueous solution. The starch-iodine solution turned deep blue in the presence of unconverted starch and the color developed was determined by measuring the absorbance at 620 nm (UV-VIS spectrophotometer, AJX-1900, Micronal, São Paulo, Brazil). The α-amylase activity was calculated by relating the absorbance of the undigested starch solution with the absorbance of the digested starch solution.

For the release assays, the NCs were redispersed into an aqueous solution using the following procedure: 2 g of NCs dispersed in cyclohexane (solid content around 3%) were added to 10 g of Tween 80 solution (1 g of surfactant in 10 g of 0.05 M PBS pH 7.4) after 30 min in a sonication bath (25 kHz) and magnetically stirred at 1000 rpm over 8 h at room temperature for the evaporation of organic solvent. After redispersion, α-amylase previously dissolved in PBS was added to the NCs. The final enzyme concentrations studied were 36, 18, 9, 0.9, and 0 mg/mL. The samples were gently shaken at 37 °C and the release kinetics of SR 101 were taken upon enzymatic degradation of the shell of the NCs. Aliquots of 1 mL were taken periodically and the enzymatic reaction was stopped by adding 0.5 mL of a 0.1 M HCl solution. The NCs were sedimented by centrifugation for 30 min at 4800 rpm (1467× *g*, MiniSpin Eppendorf, Hamburg, Germany) and the supernatant was immediately analyzed by a UV-VIS spectrophotometer (AJX-1900, Micronal) at 584 nm, as shown in Figure 2. Firstly, it was observed that the intensity of the absorbance peak and maximum absorbance wavelength of SR 101 dissolved in HCl solution were the same compared to an aqueous solution. However, after 24 h some degradation of the signal was observed, emphasizing the importance of carrying out the measurements immediately after the dissolution in HCl solution.

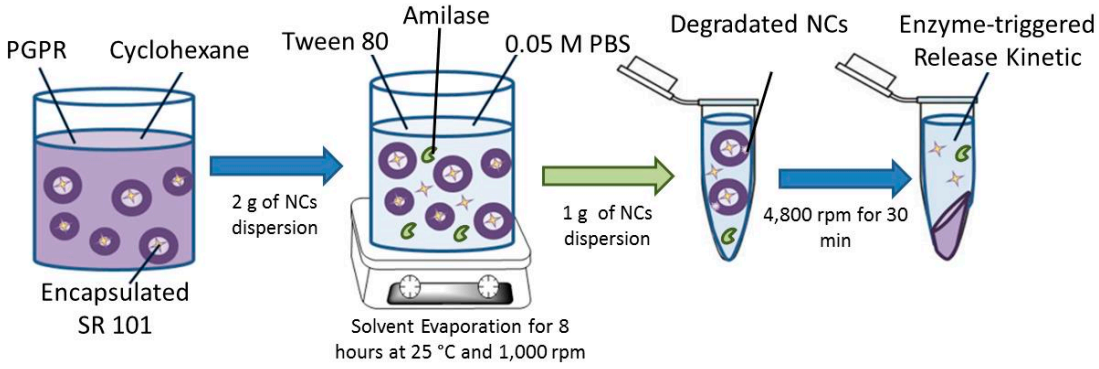

Figure 2. Schematic illustration of the procedure for determination of enzyme triggered release of SR 101 from cross-linked starch NCs.

3. Results and Discussion

Cross-linked starch NCs were prepared by interfacial polymerization firstly at 60 °C for 2 h using different types and amounts of osmotic costabilizer, as well as different surfactant, TDI, and starch concentrations. Secondly, the effect of a lower reaction temperature was investigated. Finally, shell

permeability of NCs was evaluated and impermeable shell cross-linked starch NCs were designed for enzyme-triggered release of hydrophilic compounds. The stability of the mini-emulsions of aqueous nanodroplets was investigated at 60 °C for 2 h. Results indicate that the mini-emulsions are stable during the reaction time at 60 °C. Since the final NCs are composed of a rigid shell, all of the NCs studied and stored at room temperature were stable. Although some NCs precipitated during storage, they could easily be redispersed simply by shaking by hand and no irreversible coagulation was observed.

3.1. Effect of Surfactant Concentration

The effect of surfactant concentration on the mean particle size was investigated in NCs obtained using 0.1 g of starch gelatinized in the aqueous phase, composed of 1.3 g of water and 50 mg of sodium chloride. The continuous phase of the mini-emulsion was composed of 7.5 g of cyclohexane and PGPR. The amount of PGPR varied in the range from 10 to 20 wt% related to the dispersed phase. The reaction started by adding a cross-linker solution composed of 5.0 g of cyclohexane, 30 mg of PGPR, and 120 mg of TDI. The amounts of the dispersed phase and cross-linker solution were kept constant. Table 1 summarizes the effect of surfactant (PGPR) concentration on the final particle diameter of NCs dispersed in cyclohexane and redispersed in an aqueous solution stabilized with SDS.

Table 1. Average particle size of cross-linked starch NCs prepared by interfacial polymerization in inverse mini-emulsion at 60 °C for 2 h using 120 mg of TDI. The dispersed phase was composed of 0.1 g of starch, 1.3 g of water, and 50 mg of NaCl and the continuous phase was composed of 7.5 g of cyclohexane and PGPR.

PGPR (%) *	Final Average Particle Size (nm) **	
	Dispersed in Cyclohexane	Redispersed in Aqueous Solution
10	200 ± 1	197 ± 2
15	181 ± 3	194 ± 3
20	159 ± 2	230 ± 7

* wt% related to the disperse phase; ** Mean ± SD, $n \geq 3$.

It can be observed that the mean particle size decreased with the increase of surfactant concentration for NCs dispersed in cyclohexane. This behavior was expected and the influence of surfactant concentration on particle size is well discussed in the literature [2,20]. Higher amounts of surfactant are able to provide colloidal stability to larger surface areas and, thus, smaller particles can be formed. However, when the NCs were redispersed in the aqueous solution, the mean particle size slightly increased for NCs with 15% of PGPR and sharply for that with 20 wt% of PGPR NCs, except for samples obtained with 10 wt% of PGPR, in which the particle size remained unchanged. This different behavior can be attributed to the swelling process during the redispersion step. The different swelling ability of NCs might be explained considering the interfacial polymerization mechanism. Larger particle diameters provide lower total surface area of NCs, 4.4×10^{19} nm^2 for NCs with 10 wt% PGPR compared to 5.5×10^{19} nm^2 for 20 wt% PGPR NCs and, thus, present thicker shells. Baier et al. [18] investigated the influence of surfactant concentration on the wall thickness of the cross-linked starch NC shells by SEM analysis. According to the results obtained by the authors, the thickness of the shell decreases with higher amounts of surfactant. Due to the osmotic pressure inside the NCs provided by NaCl, the swelling process is favored, increasing the particle size of the NCs with a thinner shell after redispersion in an aqueous phase, as observed for the samples obtained with 15 wt% and 20 wt% of PGPR.

FT-IR measurements were performed to investigate the shell composition and confirmed the chemical reaction between OH groups from starch and surfactant molecules with NCO groups of TDI. Figure 3a shows the spectra of cross-linked starch NCs, whose shell is composed of urethane and urea groups [18]. The carbonyl vibration at 1734 cm^{-1} and the N-H vibration at 1544 cm^{-1} are

strong evidence for the formation of urethane groups. The vibration at 1646 cm^{-1} (the carbonyl of urea groups) indicates that the side reaction of isocyanate with water occurred leading to urea units. The flat signal at 2276 cm^{-1} indicates complete consumption of NCO groups of TDI. Figure 3b shows, in detail, the spectra and the growth of the characteristic peak of the urethane group (1734 cm^{-1}) with higher PGPR concentration and smaller particle size (159 nm with 20 wt% of PGPR related to the dispersed phase). This fact might be attributed to the locus of interfacial polymerization; at the beginning of the reaction starch concentration at the interface and, thus, also that of water, was the same in smaller or larger droplets. Nevertheless, smaller droplets presented higher area/volume ratio and higher surface area led to faster interfacial reaction rates between NCO groups of TDI and OH groups from starch due the increased contact between both phases. The mobility of starch macromolecules through the shell to react with TDI at the interface is lower than that of small water molecules and, therefore, thicker shells obtained with larger particles provide more resistance. Consequently, the formation if urethane groups was favored in smaller particles. Figure 4 shows a schematic illustration of interfacial polymerization resulting in cross-linked starch NCs. Since urea bonds are stiffer and form stronger hydrogen bonding, smaller particles with lower percentages of urea bonds swell more when redispersed in water, as observed in Table 1, for NCs with 20 wt% of PGPR.

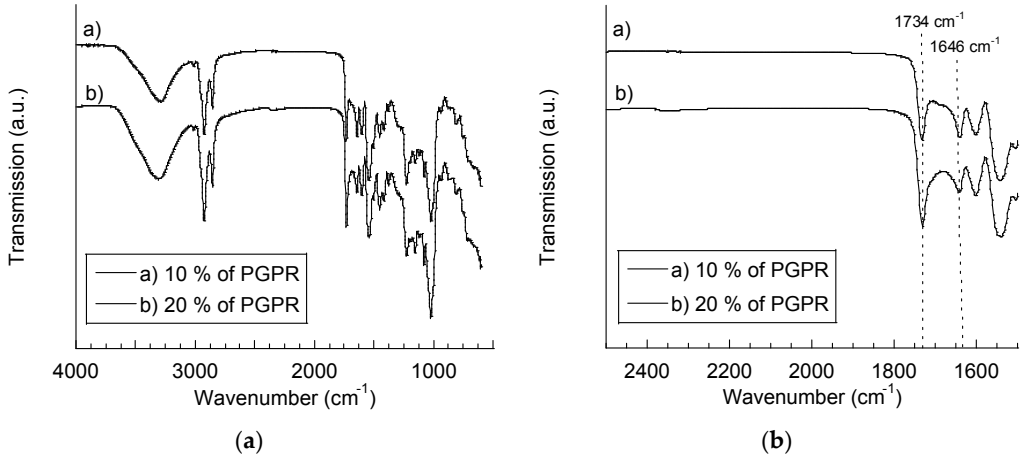

Figure 3. The effect of surfactant concentration on shell composition. Results were obtained by FT-IR using ATR mode. (**a**) Spectra between 4000 and 500 cm^{-1}; and (**b**) spectra in detail between 2500 and 1500 cm^{-1}.

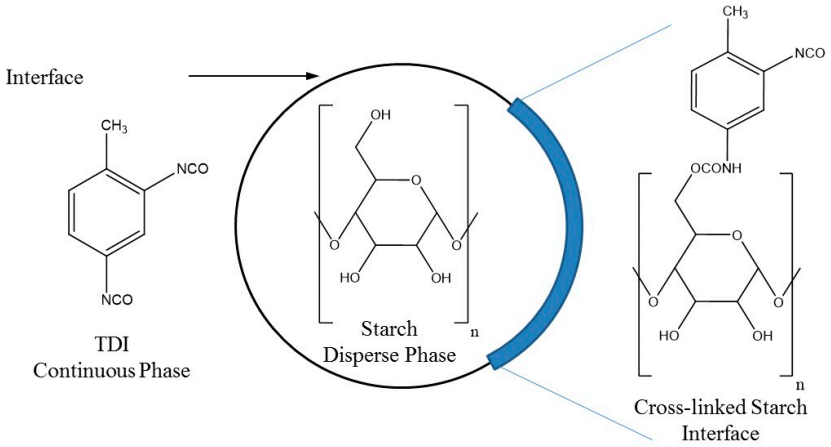

Figure 4. Schematic illustration of interfacial polymerization between NCO groups from TDI and OH groups from starch by inverse mini-emulsion.

3.2. Effect of Osmotic Agent Type

Hydrophilic salts have been used as osmotic agents (costabilizer) in order to improve the nanodroplet stability. Aqueous nanodroplets stabilized using sodium chloride and copper sulfate as osmotic agents in the dispersed phase are composed of 0.1 g of starch gelatinized in 1.3 g of water and 150 mg of PGPR as the surfactant in the continuous phase were, afterwards, cross-linked with TDI. Sodium chloride was partially replaced by $CuSO_4$, maintaining similar ionic strength. Ten milligrams of NaCl (1.71×10^{-4} mol) were replaced by 7 mg of $CuSO_4$ (4.82×10^{-5} mol).

Table 2 summarizes the formulations and shows the effect of the osmotic agent type on the average particle size of cross-linked starch NCs using different TDI amounts. It can be observed that smaller NCs were obtained using copper salt independently of the TDI concentration after polymerization. The small decrease of particle size containing $CuSO_4$ might be due to the dissociation ability, as well as to the fact that the hydrophilic salt can influence the interfacial properties of the dispersed and continuous phases and interact with the other components of the dispersed phase [23]. However, it was observed that the type and content of the salt had only a minor influence on the interfacial tension values between the phases, as shown in Table 3. In addition, while for those NCs obtained with NaCl, particle sizes remained virtually unchanged after redispersion in aqueous solution, and the particle sizes of NCs obtained with $CuSO_4$, independently of TDI concentration, increased after redispersion in aqueous solution (from about 135 nm in cyclohexane to 180 nm in water). These results indicate that these particle's shells are permeable, favoring swelling of the particle.

Table 2. The average particle size of cross-linked starch NCs prepared by interfacial polymerization inverse mini-emulsion at 60 °C for 2 h using 7.5 g of cyclohexane and 150 mg of PGPR as the continuous phase, and the dispersed phase was composed of 0.1 g of starch, 1.3 g of water, and salt.

Disperse Phase		TDI Solution	Final Average Particle Size (nm) *	
NaCl (mg)	$CuSO_4$ (mg)	TDI (mg)	Dispersed in Cyclohexane	Redispersed in Aqueous Solution
50	-	80	200 ± 2	195 ± 2
40	7	80	135 ± 1	181 ± 2
50	-	120	209 ± 1	213 ± 4
40	7	120	139 ± 2	181 ± 2

* Mean $\pm$ SD, $n \geq 3$.

Table 3. The influence of type and concentration of salt on interfacial tension values between aqueous droplets and cyclohexane with 10 wt% of PGPR related to the dispersed phase.

NaCl (mol/g) *	$CuSO_4$ (mol/g) *	γ (mN/m) **
6.58×10^{-4}	-	3.04 ± 0.09
9.21×10^{-4}	-	3.08 ± 0.03
5.26×10^{-4}	4.82×10^{-5}	3.56 ± 0.02

* Molar concentration related to water; ** Mean $\pm$ SD, $n \geq 3$.

The effect of the type of salt on the NC shell composition was evaluated using 120 mg of TDI. A comparison between FT-IR spectra of samples is shown in Figure 5. The shell composition of particles obtained using $CuSO_4$ presents a higher fraction of urethane groups, as can be observed by the growth of its characteristic peak at 1734 cm^{-1}. Smaller particle sizes of reactions using $CuSO_4$ resulted in a higher interfacial area, favoring the cross-linking reaction between starch and TDI forming urethane groups. Since the side reaction between NCO groups from TDI and OH groups from water were reduced by partially replacing NaCl by $CuSO_4$, as can be observed by the decrease of the characteristic peak of carbonyl of urea groups at 1646 cm^{-1}, as mentioned in the previous section, particles swell more after redispersion in water (shown in Table 2).

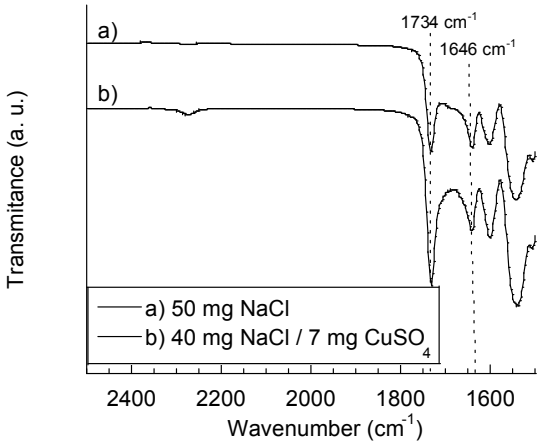

Figure 5. The effect of the co-stabilizer on the shell composition of cross-linked starch NCs prepared with 120 mg of TDI and 10 wt% of PGPR related to the dispersed phase. Results wereobtained by FT-IR using ATR mode.

3.3. Influence of the Amount of Starch

The effect of the amount of starch on the mean particle size was investigated using 50 mg of sodium chloride, 1.2 g and 1.3 g of water for 0.2 g and 0.1 g of starch, respectively, at different surfactant concentrations in the continuous phase, composed of 7.5 g of cyclohexane. The polymerization reactions were performed using 120 mg of TDI. Firstly, higher amounts of starch lead to larger particle sizes (from 200 nm to 272 nm increasing the starch amount from 0.1 g to 0.2 g, respectively, applying 10 wt% of PGPR related to the dispersed phase), as shown in Figure 6a. This fact might be attributed to the increase of the viscosity of the dispersed phase when a higher amount of gelatinized starch was used making droplet breakage more difficult during the mini-emulsion preparation. As expected, the mean average size decreased with the increase in the PGPR concentration.

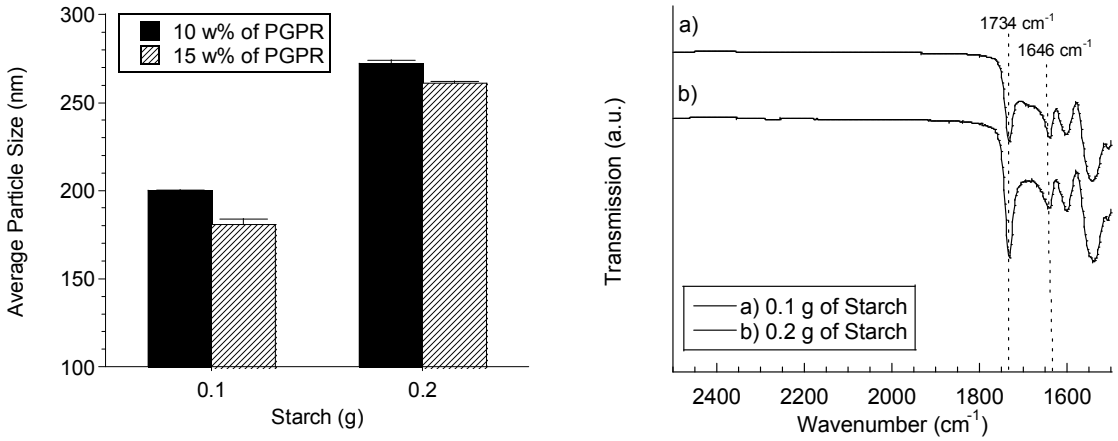

Figure 6. Effect of starch amount on (**a**) average particle size and (**b**) shell composition of cross-linked starch NCs prepared with 120 mg of TDI and 10 wt% of PGPR related to the dispersed phase. Results obtained by FT-IR using ATR mode (error bars represent standard deviation, $n \geq 3$).

The influence of the starch amount on the NC shell composition was evaluated using 10 wt% of PGPR related to the dispersed phase. A comparison between FT-IR spectra of the samples are shown in Figure 6b. Higher amounts of starch increased the fraction of urethane groups on the shell composition,

as can be observed by the growth of its characteristic peak at 1734 cm^{-1}. In addition, a higher starch concentration reduces the side reaction between NCO groups from TDI and OH groups from water, as can be observed by the decrease of the characteristic peak of carbonyl of urea groups at 1646 cm^{-1}.

3.4. Effect of TDI Concentration

Mini-emulsions prepared with 0.1 g of starch, 50 mg of NaCl and 1.3 g of water dispersed into a continuous phase composed of 7.5 g of cyclohexane and 10 wt% of PGPR related to the dispersed phase were polymerized with different amounts of TDI (varying from 80 mg to 200 mg).

Figure 7 shows the influence of the amount of TDI on the average particle size. It can be noticed that the mean diameter of NCs dispersed in cyclohexane increased with higher amounts of TDI. Nevertheless, after the NCs were transferred into the aqueous solution, the particle diameter considerably decreased (for samples prepared with 140 mg and 160 mg of TDI). Figure 8 shows a schematic illustration of a PGPR molecule adsorbed at the aqueous droplet-continuous phase interface of NCs dispersed in cyclohexane. According to Baier et al. [18], the chains of surfactant molecules are free to move in the organic continuous phase, causing the diameter variability. When NCs were redispersed into an aqueous continuous phase, the hydrophobic tail of the surfactant molecules tend to rearrange near to the NC surface. The final average particle diameters in water were around 190 nm, evidencing the absence of inter-nanocapsule crosslinking. It should be emphasized that the fraction of the dispersed phase was around 10% in volume. This content was low enough to avoid coalescence and, thus, inter-nanocapsule crosslinking.

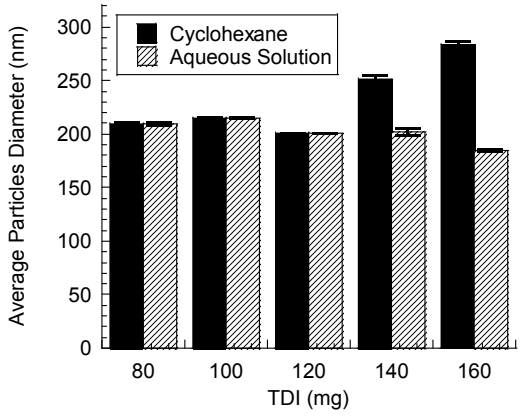

Figure 7. The effect of the amount of TDI on the average particle size using 10 wt% of PGPR related to the dispersed phase (error bars represent standard deviation, $n \geq 3$).

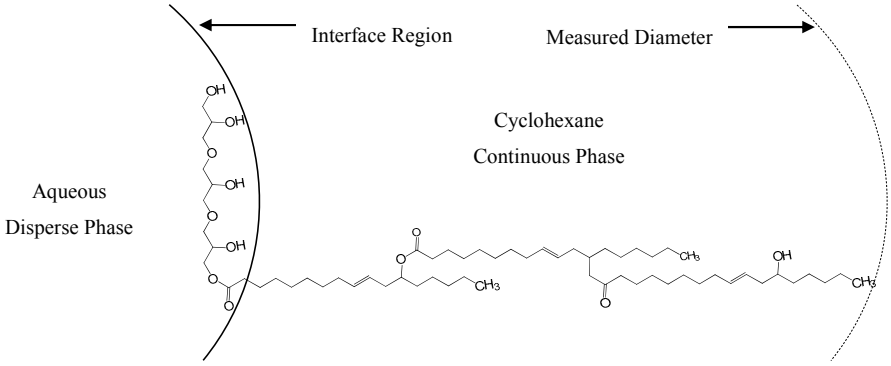

Figure 8. Schematic illustration of PGPR molecule adsorbed at the cyclohexane-aqueous droplet interface.

3.5. Effect of Reaction Temperature on NC's Shell Composition

Mini-emulsions prepared with 0.1 g of starch, 50 mg of NaCl, and 1.3 g of water dispersed into a continuous phase composed of 7.5 g of cyclohexane and 10 wt% of PGPR related to the dispersed phase were polymerized with 160 mg of TDI solubilized into 30 mg of PGPR in 5 g of cyclohexane solution at different temperatures. Figure 9 shows the influence of the reaction temperature on the capsule's shell composition. It can be observed that decreasing the temperature from 60 °C to 25 °C, a stronger NCO residual peak was observed after 24 h of reaction, due to the incomplete consumption of NCO groups of TDI at 2276 cm^{-1}. FT-IR measurements present in Figure 9 were performed using KBr pellets, instead of the ATR mode.

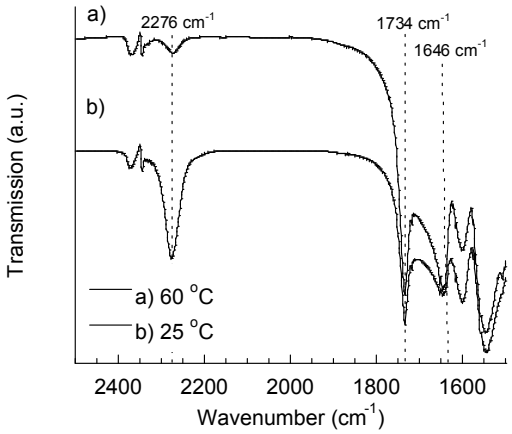

Figure 9. The influence of the reaction temperature on the composition of capsule's shells obtained by inverse mini-emulsion polymerization using 0.1 g of starch, 160 mg of TDI, and 10 wt% of PGPR related to the dispersed phase. The results were obtained by FT-IR using pellets pressed with KBr.

In addition to the fact that the reaction rate might be slower at 25 °C, the viscosity inside the aqueous droplet at a lower temperature is also higher than that at 60 °C, enhanced by the previous gelatinization of starch at 90 °C. The higher viscosity is due to the property of starch of forming a viscous gel with water when heated, followed by cooling, consisting of the gelatinized starch embedded in an interconnected network of recrystallized polymer aggregates. Since the interfacial polymerization occurs at the interface region between droplet and continuous phase, and depends on the mobility of the hydrophilic monomer inside the droplet [27], the formation of this viscous gel at 25 °C might reduce the mobility of starch inside the aqueous droplet, resulting in a lower hydroxyl concentration at the interface of the droplet and, consequently, a higher amount of residual isocyanate after the interfacial polymerization after 24 h of reaction time.

3.6. Permeability of NC Shells

The characteristics of interfacial polymerization is responsible for the final capsule morphology, composed of an aqueous core and a cross-linked starch shell. Mini-emulsions prepared with 0.1 g of starch, 50 mg of NaCl, and 1.3 g of water dispersed into a continuous phase composed of 7.5 g of cyclohexane and 10 wt% of PGPR related to the dispersed phase were polymerized with 160 mg of TDI. Figure 10 shows a SEM image of nanocapsules with an average size of around 270 nm (measured by DLS). Due to the drying and vacuum effects during the SEM measurements, the aqueous core of the NCs evaporates and the morphology appears similar to deflated balls, confirming the capsule morphology.

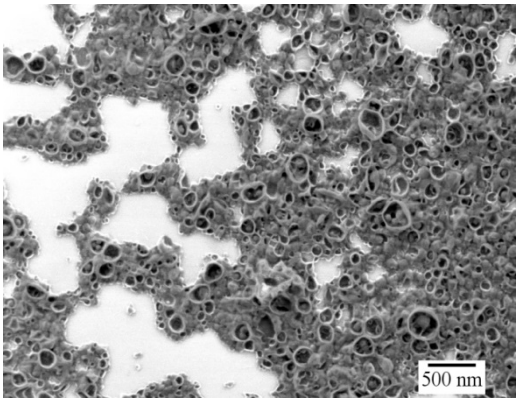

Figure 10. SEM image of cross-linked starch NCs (160 mg of TDI).

Encapsulation efficiency of hydrophilic compounds and the permeability of NC shells were assessed for nanocapsules redispersed in aqueous solution. Due to the characteristics of interfacial polymerization using inverse mini-emulsion, high encapsulation efficiencies of the hydrophilic dye SR 101 were found close to 100% for 160 mg and 80 mg of TDI, before redispersion of NCs in water (Figure 11).

The smallest amount of TDI (80 mg) did not provide an entirely sealed shell, and migration of dye to the external aqueous phase occurred leading to a lower encapsulation efficiency of SR 101 (70%) after the NCs were transferred to an aqueous solution. These results revealed that the cross-linking degree affects the ability of the capsule's shell to avoid the premature release of the hydrophilic compound.

The leakage of SR 101 after the NCs were transferred to the aqueous solution was monitored for seven days at 37 °C (Figure 12) and might be attributed to the permeability of the polymeric shell of NCs obtained with lower amounts of TDI (80 mg). Impermeable NCs were prepared using 160 mg of TDI, as shown in Figure 12, since no leakage was detected after the redispersion step of NCs from cyclohexane into the aqueous solution.

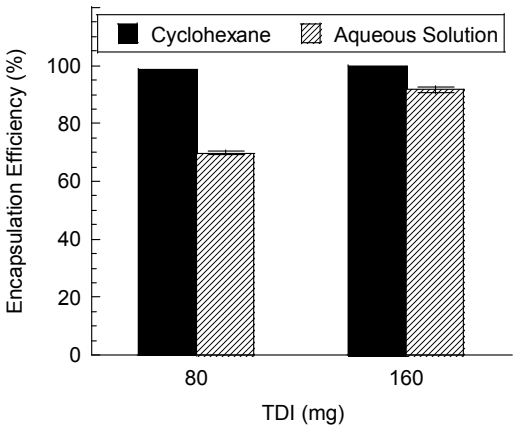

Figure 11. Encapsulation efficiency of SR 101 in NCs prepared with different amounts of TDI (error bars represent standard deviation, $n \geq 3$).

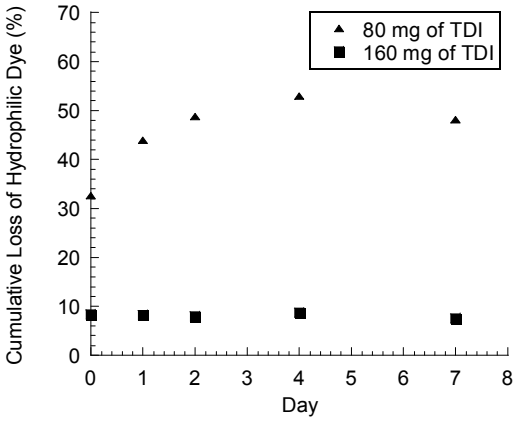

Figure 12. Cumulative loss of hydrophilic dye by leakage from the capsules to the aqueous-continuous phase.

3.7. Enzyme-Triggered Release of SR 101

The degradation assays of the cross-linked starch NCs were carried out under the same condition as used previously for the determination of the α-amylase activity (described in Section 2.2). At 37 °C and 0.05 M PBS (pH 7.4), enzymes showed an activity of 840 U/mg of enzymes.

The enzyme-triggered release kinetics of SR 101 was evaluated by enzymatic shell degradation of impermeable NCs (160 mg of TDI). The enzymatic degradation occurred using different α-amylase concentrations (36; 18; 9 and 0.9 mg/mL^{-1}). The results obtained for the maximum absorbance of SR 101 at 584 nm are shown in Figure 13.

The degradation reaction was allowed to proceed for 48 h. The maximum released SR 101 concentration was achieved after 18 h of the degradation reaction.

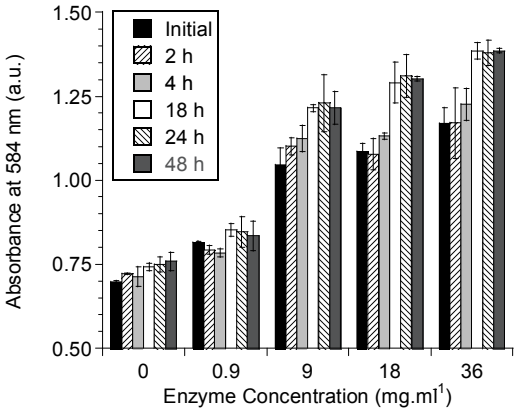

Figure 13. Release of SR 101 by enzymatic degradation using different concentrations of α-amylase (0, 0.9, 9, 18, and 36 mg/mL) (error bars represent standard deviation, $n \geq 3$).

The control sample without enzyme treatment presented maximum absorbance at around 0.750 a.u.; small increments might be attributed to damage of the capsule's polymeric shell during the centrifugation step.

The release kinetics were immediately determined after the enzyme solution was added to the NC dispersion. The higher the enzyme concentration is, the greater is the initial absorbance measured (Figure 13). These results indicate that the superficial dye entrapped at the surface of the NCs is rapidly released. After the initial period of degradation reaction (until 18 h), the SR 101 release rate slowed. The lowest enzyme concentration (0.9 mg/mL) did not show a significant release, due to its slow degradation rate.

4. Conclusions

Aqueous-core NCs were prepared via the inverse mini-emulsion technique, by interfacial polymerization between gelatinized potato starch and 2,4-toluene diisocyanate (TDI). The NCs were prepared at two different temperatures and the influence of 2,4-TDI on the polymer shell composition, particle size, and encapsulation efficiency was investigated. The ability to redisperse NCs in different continuous phases indicates the high stability of the polymeric shell. In addition, when a higher amount of TDI was used for cross-linking, the leakage of the hydrophilic dye to the aqueous phase after the redispersion in water could be readily minimized. Overall, this work presents a promising possibility for encapsulation of hydrophilic molecules with high encapsulation efficiency.

Biodegradability of NCs was demonstrated by the enzyme-triggered release of SR 101. The release kinetics were investigated using UV-Vis spectroscopy. The starch NCs were degraded by applying different enzyme concentrations. Enzyme concentrations below 0.9 mg/mL led to a slow release rate, due to the low degradation rate of the cross-linked capsule's shell.

Acknowledgments: The authors thank the financial support from CAPES—Coordenação de Aperfeiçoamento de Pessoal de Nível Superior e Tecnológico, CNPq—Conselho Nacional de Desenvolvimento Científico e Tecnológico and BMBF—Bundesministerium für Bildung und Forschung.

Author Contributions: A.M., K.L., P.H.H.A., and C.S. conceived the experiments; F.R.S. performed the experiments; and G.B. helped to analyze the data.

Conflicts of Interest: The authors declare no conflict of interest.

References

1. Vrignaud, S.; Benoit, J.-P.; Saulnier, P. Strategies for the nanoencapsulation of hydrophilic molecules in polymer-based nanoparticles. *Biomaterials* **2011**, *32*, 8593–8604. [CrossRef] [PubMed]
2. Rosenbauer, E.-M.; Landfester, K.; Musyanovych, A. Surface-active monomer as a stabilizer for polyurea nanocapsules synthesized via interfacial polyaddition in inverse mini-emulsion. *Langmuir* **2009**, *25*, 12084–12091. [CrossRef] [PubMed]
3. Crespy, D.; Stark, M.; Hoffmann-Richter, C.; Ziener, U.; Landfester, K. Polymeric Nanoreactors for Hydrophilic Reagents Synthesized by Interfacial Polycondensation on Mini-emulsion Droplets. *Macromolecules* **2007**, *40*, 3122–3135. [CrossRef]
4. Cohen-Sela, E.; Chorny, M.; Koroukhov, N.; Danenberg, H.D.; Golomb, G. A new double emulsion solvent diffusion technique for encapsulating hydrophilic molecules in PLGA nanoparticles. *J. Control. Release* **2009**, *133*, 90–95. [CrossRef] [PubMed]
5. Becker Peres, L.; Becker Peres, L.; de Araújo, P.H.H.; Sayer, C. Solid lipid nanoparticles for encapsulation of hydrophilic drugs by an organic solvent free double emulsion technique. *Colloids Surf. B Biointerfaces* **2016**, *140*, 317–323. [CrossRef] [PubMed]
6. Arpicco, S.; Battaglia, L.; Brusa, P.; Cavalli, R.; Chirio, D.; Dosio, F.; Gallarate, M.; Milla, P.; Peira, E.; Rocco, F.; et al. Recent studies on the delivery of hydrophilic drugs in nanoparticulate systems. *J. Drug Deliv. Sci. Technol.* **2016**, *32*, 298–312. [CrossRef]
7. Baier, G.; Siebert, J.M.; Landfester, K.; Musyanovych, A. Surface click reactions on polymeric nanocapsules for versatile functionalization. *Macromolecules* **2012**, *45*, 3419–3427. [CrossRef]
8. He, C.W.; Parowatkin, M.; Mailaender, V.; Flechtner-Mors, M.; Ziener, U.; Landfester, K.; Crespy, D. Sequence-Controlled Delivery of Peptides from Hierarchically Structured Nanomaterials. *ACS Appl. Mater. Interfaces* **2017**, *9*, 3885–3894. [CrossRef] [PubMed]
9. Baier, G.; Cavallaro, A.; Vasilev, K.; Mailänder, V.; Musyanovych, A.; Landfester, K. Enzyme responsive hyaluronic acid nanocapsules containing polyhexanide and their exposure to bacteria to prevent infection. *Biomacromolecules* **2013**, *14*, 1103–1112. [CrossRef] [PubMed]
10. Baier, G.; Cavallaro, A.; Friedemann, K.; Müller, B. Enzymatic degradation of poly (L-lactide) nanoparticles followed by the release of octenidine and their bactericidal effects. *Nanomed. Nanotechnol. Biol. Med.* **2014**, *10*, 131–139. [CrossRef] [PubMed]

11. Landfester, K. Preparation of Polymer and Hybrid Colloids by Mini-emulsion for Biomedical Applications. In *Colloidal Polymers Synthesis and Characterization*; Elaissari, A., Ed.; Marcel Dekker, Inc.: New York, NY, USA, 2003.
12. Liu, Z.; Jiao, Y.; Wang, Y.; Zhou, C.; Zhang, Z. Polysaccharides-based nanoparticles as drug delivery systems. *Adv. Drug Deliv. Rev.* **2008**, *60*, 1650–1662. [CrossRef] [PubMed]
13. Marto, J.; Gouveia, L.F.; Gonçalves, L.M.; Gaspar, D.P.; Pinto, P.; Carvalho, F.A.; Oliveira, E.; Ribeiro, H.M.; Almeida, A.J. A Quality by design (QbD) approach on starch-based nanocapsules: A promising platform for topical drug delivery. *Colloids Surf. B Biointerfaces* **2016**, *143*, 177–185. [CrossRef] [PubMed]
14. Rodrigues, A.; Emeje, M. Recent applications of starch derivatives in nanodrug delivery. *Carbohydr. Polym.* **2012**, *87*, 987–994. [CrossRef]
15. Humphrey, S.P.; Williamson, R.T. A review of saliva: Normal composition, flow, and function. *J. Prosthet. Dent.* **2001**, *85*, 162–169. [CrossRef] [PubMed]
16. Chourasia, M.K.; Jain, S.K. Polysaccharides for colon targeted drug delivery. *Drug Deliv.* **2004**, *11*, 129–148. [CrossRef] [PubMed]
17. Baier, G.; Baumann, D.; Siebert, J.M.; Musyanovych, A.; Mailänder, V.; Landfester, K. Suppressing unspecific cell uptake for targeted delivery using hydroxyethyl starch nanocapsules. *Biomacromolecules* **2012**, *13*, 2704–2715. [CrossRef] [PubMed]
18. Baier, G.; Musyanovych, A.; Dass, M.; Theisinger, S.; Landfester, K. Cross-linked starch capsules containing dsDNA prepared in inverse mini-emulsion as "nanoreactors" for polymerase chain reaction. *Biomacromolecules* **2010**, *11*, 960–968. [CrossRef] [PubMed]
19. Hans, M.L.; Lowman, A.M. Biodegradable nanoparticles for drug delivery and targeting. *Curr. Opin. Solid State Mater. Sci.* **2002**, *6*, 319–327. [CrossRef]
20. Asua, J.M. Mini-emulsion polymerization. *Prog. Polym. Sci.* **2002**, *27*, 1283–1346. [CrossRef]
21. Baier, G.; Friedemann, K.; Leuschner, E.M.; Musyanovych, A.; Landfester, K. PH stability of poly(urethane/urea) capsules synthesized from different hydrophilic monomers via interfacial polyaddition in the inverse mini-emulsion process. *Macromol. Symp.* **2013**, *331–332*, 71–80. [CrossRef]
22. Jagielski, N.; Sharma, S.; Hombach, V.; Maila, V.; Rasche, V.; Landfester, K. Nanocapsules Synthesized by Mini-emulsion Technique for Application as New Contrast Agent Materials. *Macromol. Chem. Phys.* **2007**, *208*, 2229–2241. [CrossRef]
23. Cao, Z.; Wang, Z.; Herrmann, C.; Landfester, K.; Ziener, U. Synthesis of narrowly size-distributed metal salt/poly(HEMA) hybrid particles in inverse mini-emulsion: Versatility and mechanism. *Langmuir* **2010**, *26*, 18008–18015. [CrossRef] [PubMed]
24. Shi, X.; Darwin, K.H. Copper Homeostasis in *Mycobacterium tuberculosis*. *Metallomics* **2015**, *7*, 929–934. [CrossRef] [PubMed]
25. Wolschendorf, F.; Ackart, D.; Shrestha, T.B.; Hascall-Dove, L.; Nolan, S.; Lamichhane, G.; Wang, Y.; Bossmann, S.H.; Basaraba, R.J.; Niederweis, M. Copper resistance is essential for virulence of *Mycobacterium tuberculosis*. *Proc. Natl. Acad. Sci. USA* **2011**, *108*, 1621–1626. [CrossRef] [PubMed]
26. Hamdi, G.; Ponchel, G. Enzymatic Degradation of Epichlorohydrin Crosslinked Starch Microspheres by α-Amylase. *Pharmac. Res.* **1999**, *16*, 867–875.
27. Morgan, P.W. *Interfacial Polymerization*; John Wiley & Sons, Inc.: Hoboken, NJ, USA, 2011; Volume 1929.